Journal of Materials Chemistry A

Accepted Manuscript

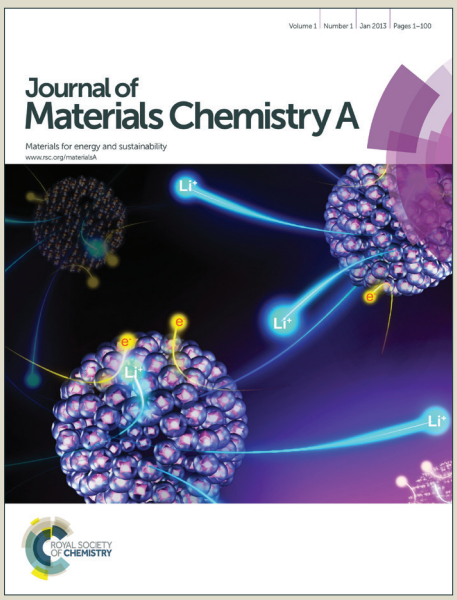

ROYAL SOCIETY OF CHEMISTRY

www.rsc.org/materialsA

Cite this: DOI: 10.1039/c0xx00000x

www.rsc.org/xxxxxx

Feature Articles

Graphene oxide nanosheet: an emerging star material for novel separation membranes

Hubiao Huang,[a] Yulong Ying,[a] Xinsheng Peng[a,b*]

Received (in XXX, XXX) Xth XXXXXXXXX 20XX, Accepted Xth XXXXXXXXX 20XX

DOI: 10.1039/b000000x

Advanced membranes that enable ultrafast permeance are very important for processes such as water purification and desalination. Ideally, an efficient ultrafast membrane should be as thin as possible to maximize the permeance, be robust enough to withstand the applied pressure and have a narrow distribution of pore size for excellent selectivity. Graphene oxide nanosheet offers an encouraging opportunity to assemble a brand new class of ultrathin, high-flux and energy-efficient sieving membranes because of its unique two-dimensional and mono-atom-thick structure, outstanding mechanical strength and good flexibility as well as its facile and large-scale production in solution. The current state-of-the-art in graphene oxide membranes will be reviewed based on their exceptional separation performance (gas, ions and small molecules). Emphases are placed on the structure of nanochannels within graphene oxide membranes, the permeance and rejection rate, and the interaction between graphene oxide sheets. The separation performance of graphene oxide membranes can be easily influenced by the state of oxygen-containing groups on graphene oxide sheets, which provides much more straightforward strategies to tune the pore size of graphene oxide nanochannels when compared to other filtration membranes. We will illustrate the review with theoretical calculations to elucidate the potential in precisely controlling the ionic and small molecular sieving and the water transport behaviour through graphene oxide nanochannels as well. This review will serve as a valuable platform to fully understand how the ions, small molecules and water transport through the laminar graphene oxide membrane as well as the latest progresses in graphene oxide separation membranes.

1. Introduction

Pressure-driven separation membranes that enable ultrafast permeance are very important in waste-water purification,[1-4] food production[5] and bio-pharmaceuticals[6] and other industries. Advanced filtration membranes with high permeance and enhanced rejection must be developed to meet the uprising environmental and energy issues. By far, membranes prepared by conventional polymeric materials have been made and exhibits good separation performance.[7, 8] But, for one hand, polymeric membranes often cannot tolerate for high temperature and corrosive medium like strong acids/alkaline and organic solvents;[9-11] For another hand, the applied pressure may cause the compaction of polymeric membranes, which will lead to a denser structure (with smaller pores). As a consequence, the permeance of such membranes will dramatically decline.[11, 12] Porous ceramic membranes such as Al_2O_3, TiO_2 and ZrO_2, make up for the aforementioned shortages of polymeric membrane.[13, 14] They have good chemical resistance,[15] high flux and rejection rate.[16, 17] But ceramic membranes are very expensive, and very brittle and easy-broken especially when a pressure is exerted on them in the real pressure-driven separation processes.[4] In addition, the fabrication of ceramic membranes is typically conducted by sintering and sol-gel method.[14, 18] These processes are time-consuming and complex. Therefore, ceramic membranes are normally confined to laboratorial and some special uses.

Recently, significant interests in carbon-based materials have rapidly grown because of theirs easy accessibility, good mechanical property, chemical inertness, environmental friendly and so forth.[19-25] Many scientists initially believe that carbon nanotube is a very compelling candidate for membranes assembly, owing to its unique one-dimensional hollow structure with open ends and very strong mechanical strength[22, 26]. Most recent theoretical studies reveal that pressure-driven gaseous and liquid flow could freely transport through the frictionless inner cores of carbon nanotubes. The fluxes of gases like N_2, CO_2, Ar, H_2, and CH_4 is about 15-30 folds higher than that predicted from Knudsen diffusion kinetics.[26] And the liquid, water for instance, is over 4 orders of magnitude larger than "no-slip" hydrodynamic flow predictions.[27-30] However, it is an enormous technical challenge to assembly vertically aligned carbon nanotubes arrays with high density in a large scale and therefore membranes constructed by carbon nanotubes are basically limited to theoretical studies, despite many attempts being made.[26, 31] Another carbon-based material-diamond-like carbon (DLC), which is amorphous carbon with significant sp^3 bonded carbon atoms, is likewise assumed to be an ideal material for assembling filtration membrane, due to its

high mechanical hardness and chemical inertness.[19] DLC membrane prepared by Karan *et al*.[23, 32] has been demonstrated superior separation performance for organic solvents. Unfortunately, despite its excellent separation performances, the applicability of DLC membranes in real separation application is still limited because of equipment size and energy utilization efficiency, [19, 33] which encourages people to develop more applicable and economical membranes.

The advent of graphene and its derivative opens a brand new era for assembling membranes with perfect separation performances, because of its unique mono-atomic thickness, two-dimensional structure, high mechanical strength and chemical inertness. [34, 35] Theoretical studies indicate that single-layered porous graphene is of great potential in seawater desalination,[36] gas separation[37] and drinking water production.[38] But, how to precisely control the pore size on the graphene is a tough technical challenge. In addition, mono-layered porous graphene membranes cannot be available in a large scale and tolerate high pressure exerted on such membranes in the real pressure-driven separation applications.[34, 39]

To address this problem, several excellent filtration membranes constructed by graphene oxide (GO) sheets have been reported very recently and opened up an exciting direction in separation membranes because of its facile and large-scale production in solution.[40, 41] Laminar GO membranes assembled by using micrometer-sized GO sheets via vacuum filtration exhibit several distinguished characteristics, including hydrophilism, outstanding mechanical strength and good flexibility, which make GO a very promising candidate for water purification and sieving.[24, 42-44] However, the permeation through these GO membranes via diffusion remains insufficient to allow them to compete with commercial pressure-driven ultrafiltration membranes. Qiu[45] *et al.* first reported pressure-driven separation performance of the thermally corrugated GO membranes with an obviously elevated permeance of 45 L m^{-2} h^{-1} bar^{-1}, due to the presence of obvious microscopic wrinkles within the GO membrane, which hints that numerous well-defined channels is supposed to be favorable for elevating the separation performance of GO membranes.[5] Recalling the control of the pore size or porosity of GO membranes, we have already made remarkable achievements, yet there is still an urgent need for improving techniques of GO membrane design and assembly to attain outstanding GO membranes with high permeance, excellent selectivity and stable performance to meet growing demands therein.[46, 47] For this reason, we recommend interest readers should take note of a recent critical comment on GO membranes for ionic and molecular sieving.[48] The current state-of-the-art in GO membranes will be reviewed based on their exceptional separation performance (gas, ions and small molecules). Emphases are placed on the structure of nanochannels within GO membranes, the permeance and rejection rate, the interaction between GO sheets and ions/molecules and the way of water transport in GO nanochannels. It is worth noting that the separation performance of GO membranes can be easily influenced by the physiochemical state of oxygen-containing groups on GO sheets, which provides much more straightforward strategies to tune the pore size of graphene oxide nanochannels when compared to other filtration membranes. This critical review aims not only to understand physicochemical properties of fully wetted GO membranes, but, for the first time, provide a systematic discussion of graphene oxide membrane from the pressure-driven separation application perspective as well as the latest progress in GO membranes with enhanced separation performance.

2. Graphene oxide membrane

2.1 Structure of graphene oxide nanosheets

GO is a mono-layer-thick and two-dimensional nanomaterials. The precise chemical structure of graphene oxide sheets has been debated for decades with uncertainty pertaining to both the type and distribution of oxygen-containing functional groups, and even to this day no unambiguous model exists. Nevertheless, the most compelling and widely recognized structural model of GO is known as Lerf-Klinowski model.[49, 50] According to this model, several oxygen-containing groups are decorated to the basal planes and edges of GO, including epoxy, hydroxyl and carboxyl groups.[51] Because of the existence of these oxygen functional groups, GO exhibits a series of exciting properties. On the one hand, GO can be readily dispersed in water medium and can form well-dispersed aqueous colloids without the help of any surfactant or stabilizing agent, [40, 46, 52] which allows GO to be readily manipulated in aqueous solutions and makes it much easier to assembly thin films. For the other hand, these submicrometer-sized GO sheets are highly negatively charged when dispersed in water, as a result of ionization of the carboxyl groups on the edges of GO sheets.[47] In addition, those carbon atoms being bonded with oxygen atoms in the form of epoxy, hydroxyl and carboxyl groups tend to form amorphous regions due to distortions from the high proportion of sp^3 C-O bonds (~40%), resulting in nanoscale wrinkles and structural defects in basal plane of GO sheets,[41, 46, 53] which provide primary passages for water transport when GO sheets are assembled into membranes.[45] Besides, these functional oxygen-containing groups provide many reactive handles for a variety of surface-modification reactions, which can be used to develop a series of functionalized GO-based membranes with much enhanced separation performance.

2.2 Preparation of graphene oxide membrane

The ionization of carboxyl acid and phenol hydroxyl groups made the surface of GO sheets bear a certain number of negative charges that has been demonstrated by zeta potential tests.[46, 47, 52] Due to the strong electrostatic repulsion between these negatively charged layered GO sheets, single-layered GO sheets were avoided from overlapping or even corrugating for months, but inclined to fold and wrinkle at edges to resist collapsing into multilayers. Once GO sheets are assembled into membranes, the individual GO sheets are interlocked in a parallel manner and form mechanically-robust GO membranes. The as-prepared GO membranes can be easily transferred to another substrates.

2.2.1 Drop-casting

The assembly of GO membranes via drop-casting is described as follows: GO colloidal suspension was drop-casted onto a substrate with smooth surface such as silica or paper and dried at room temperature. A piece of freestanding and uniform GO

membrane was subsequently peeled off from the underlying substrate.[43, 54]

2.2.2 Spraying- or spinning-coating

GO colloid suspension is spin- or spray-coated on a smooth substrate such as Cu foil or polymeric support to fabricate thin and uniform GO membranes.[24, 55] For example, when GO suspension is placed on a Cu foil support, in order to reduce the deposition duration, the substrates were usually heated to ~50°C in the process of spin-coating. Freestanding GO membranes were obtained by etching away the central part of the copper foil in nitric acid. Finally, the membranes were cleaned by deionized water and dried on a hot plate (<50°C). This dense stacking occurs because the face-to-face attractive capillary forces created by the spray- or spin-coating can overcome the repulsive forces between the edges of GO sheets. Therefore, the initial deposition is governed primarily by capillary interactions between the GO sheet faces, other than the electrostatic forces between the GO edges.

2.2.3 Langmuir−Blodgett (LB) method

Typically, the basal plane of mono-layered GO sheets is composed by both hydrophobic nonoxidized regions (sp^2-bonded carbon atoms network) and hydrophilic oxidized ones (sp^3-bonded carbon atoms network).[24] Therefore, GO sheets can be deemed as amphiphilic material.[56] For LB technique for assembling GO membranes, the trough was first carefully rinsed with chloroform and then filled with de-ionized water. GO suspension was slowly spread onto the water surface with a speed of 100 µL/min using a glass syringe to a total volume of 8-10 mL. Surface pressure of GO film was monitored using a tensiometer. A GO film with faint brown color could be observed at the end of the compression. The GO monolayer was transferred by vertically dipping the substrate into the trough and then slowly pulling it up (2 mm/min). Bi- and trilayers of GO films were prepared by drying the as-formed films in an oven and then depositing another layer of GO under the same condition.[57] Through the LB technique, the layers and thickness of GO membranes can be readily controlled.

2.2.4 Vacuum filtration

Vacuum filtration is the most common and straightforward route towards the large scale fabrication of GO membranes. Diken *et al*.[51] and Putz *et al*.[58] proposed possible mechanisms for the formation of paper-like GO membranes. Compression induced by vacuum sucking was responsible for aligning the GO sheets perpendicular to the flow direction and narrowing the inter-spacing between the oriented GO sheets, achieving a higher degree of paralleled arrangement throughout the structure. It is worth noting that this process didn't change the physiochemical properties of GO, because the interactions between the very large aspect ratio compliant sheets GO sheets are electrostatic repulsion, van der Waals attractive forces and hydrogen bonds and no covalent bonding was formed.[51] GO membranes likewise bear a certain number of negative charges and present excellent hydrophilic property.[45-47, 59] Typically, the thickness of GO membranes largely depends on the volume of GO suspension filled into the cell of vacuum filtration system. In addition, GO membranes prepared by filtration are usually deposited on microporous polymeric membranes. The microporous polymeric support is selected to optimize both surface roughness and wet-ability to achieve a homogeneous GO membrane.

3. Separation performance of graphene oxide membrane

Unlike polymeric or ceramic membranes, layered GO membranes possess a series of distinguished properties, including its facile and large-scale production in solution, hydrophilism, outstanding mechanical strength and good flexibility,[51, 60, 61] which other membrane materials cannot compete with. The interconnected tortuous path for water molecules, ions, small organic molecules, and nanomaterials transportation are primarily composed by the randomly distributed nanoscale wrinkles, inter-spacing strutted by functional oxygen groups (hydroxyl, carboxyl and epoxy groups aforementioned) and nanopores induced by structural defects on basal plane of GO sheets.[45, 46, 62] Recent studies have demonstrated that GO membranes exhibit a huge potential in gas, ions and small molecules separation.

3.1 Gas separation

GO membranes present an excellent opportunity to be employed as a barrier to encase organic solvents or gases. Nair and co-workers tested the permeance of several gases, including He, H_2, N_2, and Ar, through metal containers capped with GO membranes with thicknesses *h* from 0.1 to 10 mm.[24] The leakage rate was monitored by the variations of inner pressure of sealed containers over a period of several days. The results revealed that no noticeable reduction in pressure was observed for any tested gas including He, H_2, N_2, and Ar, suggesting that submicrometer-thick GO membranes were completely impermeable to these

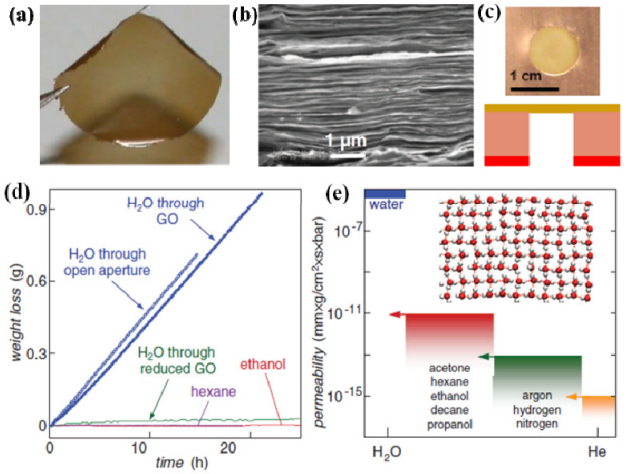

Fig. 1. *(a) Photo of a 1-mm-thick GO film peeled off of a Cu foil. The film's cross-section SEM image; (c) mounted on copper hole for separation test; (d) water vapour permeates through a sealed GO film (h ≈1 mm; aperture's area ≈1 cm²). (e) Permeability of GO paper with respect to water and various small molecules (arrows indicate the upper limits set by our experiments). (Inset) Schematic representation of the structure of monolayer water inside a graphene capillary with d = 7 Å. Adapted with from ref. 24 with permission from The American Associate for the Advancement of Science.*

tested gases, which is similar to that of the continuous graphene

monolayers. In that case, the mono-layered graphene sheet blistered under a small overpressure.[63] Besides, Nair *et al.* employed weight-loss measurements to evaluate the permeation rate for liquid substances such as water and organic solvents vapors as shown in **Fig. 1**. Likewise, organic solvents like ethanol, hexane, acetone, decane and propanol were added into metal chambers with the aperture sealed by GO films. No weight loss could be detected with accuracy of <1 mg in the measurements lasting several days. However, a huge weight loss was observed when the container was filled with water unexpectedly, which is more than 10 orders of magnitude higher than He. Further studies revealed that the permeation rate of water vapor through the container sealed by GO films is as fast as an open aperture. Nair *et al*. attributed this fast transport of water vapor to low-friction nanocapillaries formed by empty inter-spacing (estimated as ~5 Å) between nonoxidized regions of GO sheets, which is sufficient to allow mono-layered water to transport through. Whereas Boukhvalov and co-workers reported that anomalous water permeation through GO membrane is due to the formation of ice bilayer inside graphene regions of GO membranes and their melting behaviors owing to their optimal interlayer distance.[64] In addition, the permeation rate of mixture gases was also tested. For example, when the mixture is He and water vapor, the permeation of He is still too minimal to compete with that of water vapor because the intercalating water at least impedes larger molecules from moving through nanocapillaries. Therefore, GO membranes had a huge potential in the production of leak-tight membranes. It is noted that the inter-spacing of GO films is quite sensitive to humidity.[59] As for the fully wetted GO membranes, the space between adjacent GO sheets could expand to more than 1 nm according to the XRD results.[46] But the GO membranes became very easy-broken and couldn't stand for relatively high applied pressure when placed for gas leakage test. More investigations are needed to address whether the variation of interlayer spacing of GO films in dry/wet state has impact on the permeation rate of various gases. Very recently, Kim *et al.*[65] believe that the prime paths in GO membranes for gas transport are composed by two individual parts: 1) defects on GO sheets, such as tears and holes; 2) interlayer spacing formed by irregular stacking due to these corrugations, wrinkles and ripples. The transmembrane pressure, in fact, acts as a key role to decide whether thin GO membranes should be permeable to small gases or not. In other words, if sufficient transmembrane pressure is exerted on GO membrane to overcome the energy barriers to pore entry and diffusion within nanopores or nanochannels, thin GO membranes could be permeable to other gases. The gas separation tests results (**Fig. 2**) reveal that gas transport via Knudsen diffusion[66] is determined by the effective pore size of the GO membrane as well as the free path length of the gases. As expected, the permeation rate of most of tested gases through the dry GO membranes depends on differences in their molecular weights (**Fig. 2a**), except for CO_2. This is because the polarity of the individual C-O bonds in the molecule can interact with polar groups, particularly the carboxyl acid groups at the edges of GO sheets, consequently retarding CO_2 transport in the nanochannels or nanopores in GO membranes (**Fig. 2b**). However, when the humidity or preparation method changes, GO membranes are conversely in favor of CO_2 transport and block other gases, resulting in excellent selectivity of mixed gases. The separation

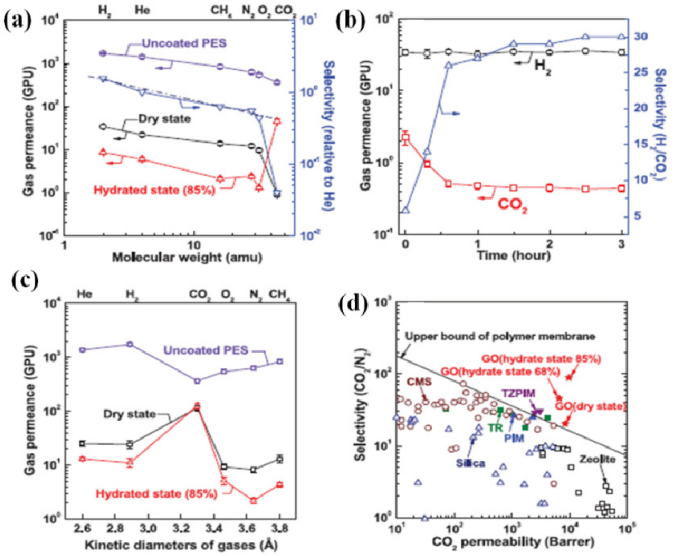

Fig. 2. *(a) Gas permeances of GO membranes as a function of molecular weight (method one; dashed line represents the ideal Knudsen selectivity) under dry and humidified conditions. (b) H_2 and CO_2 permeances and H_2/CO_2 selectivity of method one GO membranes as a function of permeation time. (c) Gas permeances of GO membranes as a function of kinetic diameter (method two) under dry and humidified conditions. (d) Relation between CO_2 permeability and CO_2/N_2 selectivity of method two GO membranes under dry and humidified conditions. Error bars indicate the SD of all raw data. Reproduced with from ref. 65 with permission from The American Associate for the Advancement of Science.*

performance of GO membranes in this situation is obviously better than that reported for CO_2 for polymeric membranes, including thermally rearranged (TR) polymers,[67] polymers of intrinsic microporosity (PIM),[68] and inorganic membranes.[69] Also, Li *et al.*[70] demonstrated that GO membranes of 1.8 nm in thickness reproducibly fabricated by a facile filtration approach alternatively showed extraordinary selectivity of H_2 from H_2/CO_2 and H_2/N_2 mixture, which are one to two orders of magnitude higher than those of the state-of-the-art microporous membranes.[71]

3.2 Ions selectivity

Although nanoporous graphene films have demonstrated potential use in gas separation,[37, 72-75] ions selectivity[76] as well as water desalination[36, 38] according to molecular simulation (MD) results, it is still a huge challenge to achieve large-area, high quality and single-crystal graphene films, even though many attempts have been made.[77-79] In addition, the immature techniques of introducing nanopores into graphene basal plane also limit the application of nanoporous graphene films in separation and sieving, especially in pressure-driven processes. Freestanding GO membranes, however, overcome these shortages of nanoporous graphene films aforementioned and enable us to perform ions separation on an experimental level. Sun *et al.*[43] found that sodium salts could freely and quickly pass through GO membranes, but some heavy-metal ions, Cu^{2+} for example, are entirely blocked, which is typically characterized by the

conductivity of the filtrates, the rentates and the feeds. The specific mechanism of the selective penetration properties of GO

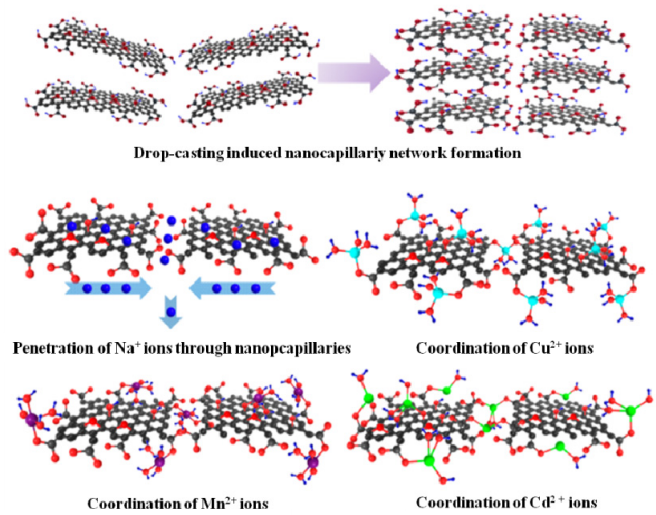

Fig. 3. *Schematic diagrams of GO membrane and the interaction with different ions. Reproduced from Ref. 43 with permission from American Chemical Society Publications.*

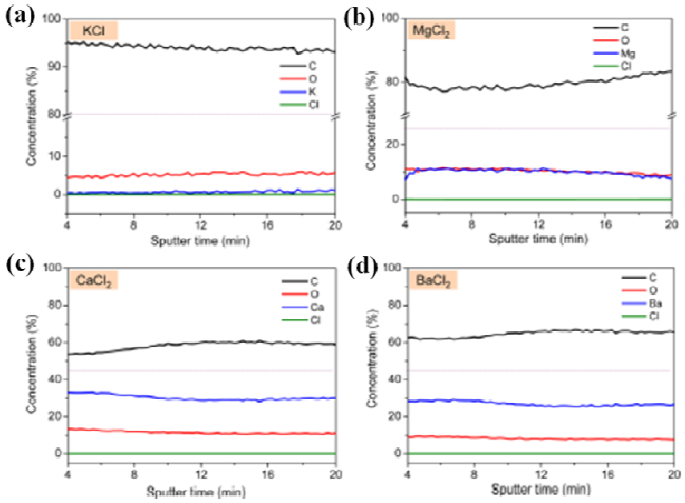

Fig. 4. *AES spectra for GO membranes after the penetrations of (a) KCl, (b) $MgCl_2$, (c) $CaCl_2$, and (d) $BaCl_2$ solutions. The sputter rate is 13 nm/min for SiO_2. Reproduced from Ref. 54 with permission from American Chemical Society Publications.*

membranes was also investigated by Sun and co-workers. The pore size of nanochannles within fully wetted GO membrane is in the range from 3 to 5 nm, which is demonstrated by the previous work.[45-47] The very tiny molecules and nanoparticles could readily accommodate and migrate along with these interconnected nanochannels. But the permeation of some heavy-metal ions, including Cu^{2+}, Cd^{2+} and Mn^{2+}, is significantly slower, even totally blocked, than that of sodium salts due to the strong interactions between these heavy-metal ions and oxygen-containing groups (**Fig. 3**), other than physical absorption. In addition, in the case of alkali and alkaline earth cations, the GO membranes also present selective permeation of cations because of the different strength of cations-π interactions. **Fig. 4** indicates the Auger electron spectra (AES) of GO membranes after the permeation tests of Cl^-, K^+, Mg^{2+}, Ca^{2+} and Ba^{2+} aqueous solutions, suggesting that the velocity of the transport rate of these cations is different, which could facilitate the separation of specific ions from wastewater. Also, it provides a promising approach to seawater desalination and the possibility of modeling the ion transport of cellular membrane using GO membranes by diffusion process.

3.3 Small molecules and nanomaterials separation

As a result of the extremely tiny nanocapillaries formed by the non-oxidized regions of GO sheets, dry GO membranes exhibit a series of advantages in gas-leakage test[24] and ions selectivity[43, 54] in the diffusion process. The typical pore size of such nanocapillaries is expected as 0.7 nm according to the previous work.[24] However, as for the fully wetted GO membranes, the situation is totally different. Hydrophilic oxygen-containing groups, including hydroxyl, carboxyl and epoxy, can absorb plenty of water molecules, resulting in expansion of intersheet spacing of laminar GO membranes to more than 1 nm, which will definitely increase the effective pore size of nanochannels within GO membranes.[46, 47] Besides, the pressure-driven separation process does, on one hand, accelerate the permeation rate of water flow and therefore enhance the separation efficiency. On another hand, the pressure exerted on GO membranes is sufficient to overcome the hydrogen bonds between oxygen-containing groups of GO sheets and water molecules. Consequently, the nanochannels within fully wetted GO membranes are composed by: 1) wrinkles, 2) inter-spacing and 3) few nanopores caused by structural defects.[46] According to molecular sieving mechanism, the effective pore size of nanochannels within micrometers-thick GO membrane is in the range from 3 to 5 nm. Qiu *et al*. first proposed that the corrugations within fully wetted GO membranes provide typical path to allow liquids and small nanoparticles to transport. The amplitude of the corrugations can be indirectly reflected by the water permeation test of GO

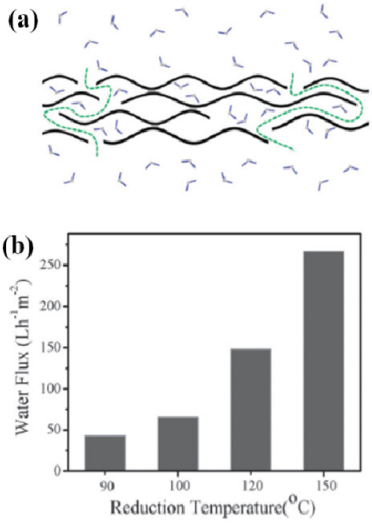

Fig. 5. *(a) Schematic of water flowing through a corrugated chemically converted graphene (CCG) membrane. The dashed line indicates possible water flow paths. (b) Water fluxes of the membranes of CCG sheets prepared at various temperatures with same amount of CCG. Reproduced from Ref. 45 with permission from The Royal Society of Chemistry.*

membranes as shown in **Fig. 5**. Of particular interest is that the

number of these corrugations can be easily controlled by the hydrothermal treatment of GO suspension and thus affect the separation performance of the target GO membrane (**Table 1**). Inspired by this novel approach, Huang *et al.*[47] found that salt concentration, pH and applied pressure also have great influence in separation performance of

Table 1. *The hydrothermal treatment of GO suspension and thus affect the separation performance of the target GO membrane. Reproduced from Ref. 45 with permission from The Royal Society of Chemistry.*

	Pt NPs rejection	Au NPs rejection	Pore size/nm
90 °C-CCG	✗	✗	<3
100 °C-CCG	✓	✗	3–13
120 °C-CCG	✓	✗	3–13
150 °C-CCG	✓	✓	>13

GO and offer much more straightforward strategies to tune the separation performance of GO membranes. As mentioned before, the physiochemical properties of GO do not change when individual GO sheets are assembled into membranes. Therefore, the fully wetted GO membranes still bear a certain number of negative charges and these nanochannels are thus quite susceptible to any changes in the charges on GO sheets, giving rise to a remarkable impact on the zeta potential of GO sheets. When soluble electrolytes are introduced into the cell upon the GO membrane, it could result in shrinking of nanochannels within GO membranes and sharply reducing the water permeance because of ionic screening effect. Likewise, the surface charge density of GO sheets also strongly depends on pH value based on the zeta potential tests of GO suspension with different pH value due to the protonation or deprotonation of carboxyl acid groups on the edges of GO sheets. The pH-dependent alternation of nanochannels is indirectly confirmed by the separation performance. At high or low pH, the water permeation rate is extremely low and rejection rate of Evans-blue (a dye ~ 3 nm) is obviously enhanced because of the combination of protonation (or deprotonation) of carboxyl groups and ionic screening effect, which are responsible for the variation of the effective pore size of nanochannels within GO membranes. In addition, the GO nanochannels experience series of reversible alteration when a pressure is exerted on the GO membranes. Of course, there are plenty of other effective approaches to improve the separation performance of GO membranes as will be discussed latter.

4. Improved separation performances of graphene oxide membranes

Although the water permeance of GO membranes can reach 71 L m^{-2} h^{-1} bar^{-1}, it is still needed to enhance to meet the industrial demands.[46] In order to further improve the separation perforamcne of GO membranes, significant efforts have been devoted to develop highly efficient GO membranes. Three categories of GO membranes, even though some of them are only proposed, will be discussed in the listed subchapters below.

4.1 Nanoporous graphene oxide membranes

The perfect single-layered graphene sheet is demonstrated to be impermeable to gases as small as H_2 or He.[63] This is due to the fact that the electron density of its aromatic rings is substantial enough to block any atoms, ions and molecules trying to transport through these rings.[37] Recently, waves of discoveries, using either electron beams, bottom-up synthesis techniques, diblock copolymer templating, helium ion beam drilling or chemical etching, [35, 80-83] have been made to achieve nanoporous graphene with high selectivity and extremely fast permeability. The as-prepared ultrathin nanoporous graphene sheets have higher porosity and a more precise pore size distribution. Based on MD

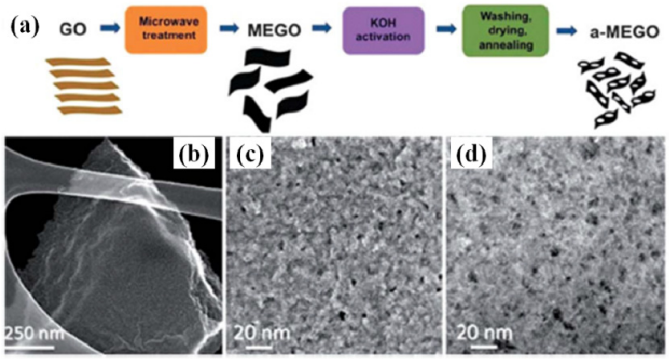

Fig. 6. *(a) Schematic showing the microwave exfoliation/reduction of GO and the following chemical activation of microwave exfoliated GO (MEGO) with KOH that creates pores while retaining high electrical conductivity. (b) Low magnification SEM image of an activated MEGO (a-MEGO) piece. (c) High-resolution SEM image of a different sample region that demonstrates the porous morphology. (d) ADF-STEM image of the same area as (c), acquired simultaneously. Adapted with from ref. 85 with permission from The American Associate for the Advancement of Science.*

simulations and first principles density functional theory calculations results, nanoporous graphene with well-defined pores has a wide of potential applications in fields such as water desalination, DNA sequence, ion selectivity and gas separation.[34, 36, 37, 39, 74, 84] Inspired by this approach, we can likewise "drill holes" on GO sheets and then assemble nanoporous GO membranes for the purpose of improving the separation performance of GO membranes. In this section, we will focus on the methods of introducing in-plane nanopores on GO sheets.

It is well known that strong alkali solution such as KOH is deemed as a very efficient chemical active agent, which is widely utilized in preparing for porous carbon materials. Very recently, Zhu *et al.*[85] found that exfoliated GO activated by KOH could form a large number of well-defined pores on GO sheets (**Fig. 6**). The effective pore size of such nanoporous GO membranes is in the range from 0.6 to 5 nm, which is comparable to that of pristine GO membranes (3~5 nm). Despite many nanopores formed in this activation process by KOH, the activated GO sheets become less hydrophilic because of the fact that certain oxygen-containing groups are removed in this process. But it is still possible to fabricate uniform membranes with much more water-transport path and therefore accelerate the separation process. Alternatively, Radich and co-workers found RGO could be readily oxidized when irradiated with H_2O_2 and Au nanoparticles, which therefore could give birth to both wrinkles and nanopore of 5~100 nm in diameter (**Fig. 7**).[86]

It is worth mentioning that these approaches to make nanopore on GO sheets proposed here might change the physicochemical

properties may change such as the lateral size of GO, structural defects and hydrophilic property when GO sheets are treated in the harsh conditions. Whereas, it might be very promising methods to achieve nanoporous GO membrane with extremely high permeability and excellent selectivity.

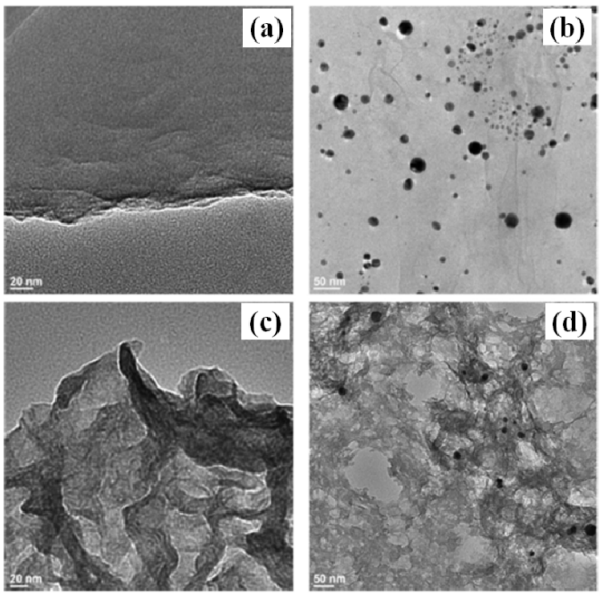

Fig. 7. *TEM images of (a) RGO, (b) Au + RGO, (c) H_2O_2 + RGO, (d) Au + H_2O_2 + RGO after 2 h irradiation time. Reproduced from Ref. 86 with permission from American Chemical Society.*

Interestingly, Ying *et al*. have reported that nanopores could be readily introduced into the basal plane of GO sheets by re-oxidation of GO with strong oxidizing agent such as $KMnO_4$. Not only do these nanopores increase the effective path for water molecules, but also greatly shorten the distance of water transporting through GO membranes (**Fig. 8**).[87] The separation test results reveal that such mesporous GO membranes present an excellent rejection for evans-blue molecules (88.5%) and a fast water permeance of 191 L m^{-2} h^{-1} bar^{-1} that is almost three times higher than that of pristine GO membranes. Likewise, nanochannels within such mesporous GO membranes also exhibit reversible elastic property when extra pressure is exerted on such membranes.

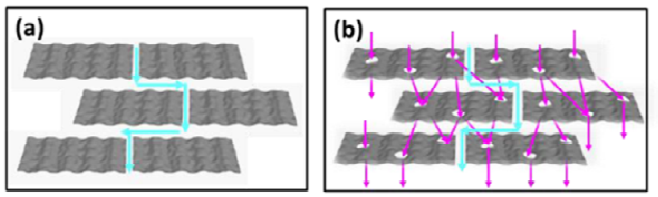

Fig. 8. *Schematic view mass transport through (a) pristine GO and (b) mesoporous GO membranes. Reproduced from Ref. 87 with permission from The Royal Society of Chemistry.*

4.2 Chemically cross-linked graphene oxide membrane

Despite optimum separation performance of pristine GO membranes, the mechanical strength of fully wetted GO membranes cannot compete with that of other nanofiltration membranes, such as polymeric membranes and zeolite membranes. The functional groups (particularly carboxyl groups) on GO nanosheets not only offer itself good hydrophilism, but provide active sites for further chemical functionalization to meet specific demands such as surface charges, mechanical strength as well as surface morphologies. Besides, the intercalated organics or some ions between laminar GO membranes, for one hand, can partially expand the inter-spacing of adjacent GO sheets. For another hand, these intercalation materials also act as barriers to form new channel. All of them are in favor of enhancing the water permeability. In the previous studies, the primary purpose of the synthesis of chemically cross-linked GO membrane is to improve the mechanical properties of GO membranes. For example, Park and co-workers found that the

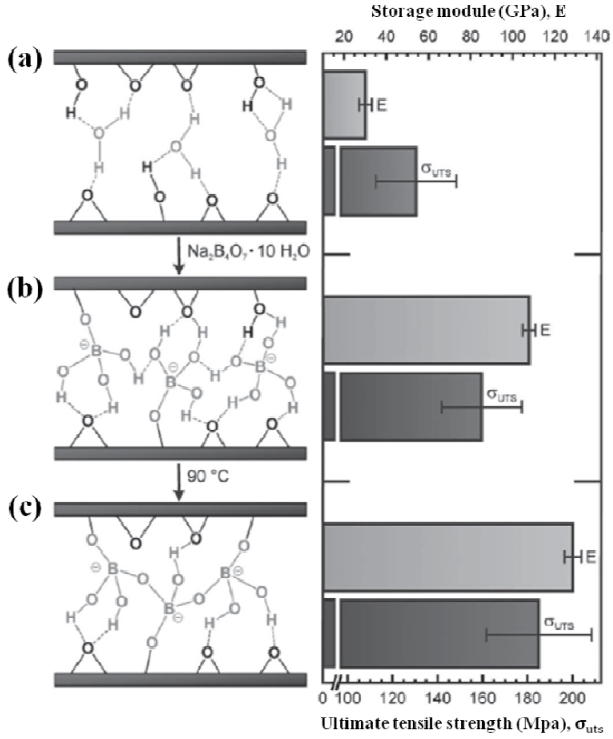

Fig. 9. *Left: Schematic illustration of (a) Water molecules form hydrogen bonds with epoxide and hydroxyl groups to bridge nanosheets in an unmodified graphene oxide thin film. (b) In addition to forming hydrogen bonds, borate anions react with surface-bound hydroxyl groups to give borate orthoester bonds, improving the mechanical properties beyond those of the unmodified film. (c) Thermal annealing drives the formation of more covalent bonds within the intersheet gallery, affording an ultra-stiff thin film. Right: Mechanical properties of respective films, demonstrating that ultra-stiff films are only obtained after annealing borate-modified films under a flow of dry N_2. Reproduced from Ref. 88 with permission from John Wiley and Sons.*

mechanical strength of paper-like GO membranes modified with a small amount of Mg^{2+} and Ca^{2+} presents a significant enhancement. The mechanical stiffness and fracture strength of newly stacked GO membranes increase 10~200% and 50% in comparison with the pristine GO membranes, respectively. This is due to the fact that oxygen functional groups on the basal planes of the sheets and the carboxylate groups on the edges can both bond to Mg^{2+} and Ca^{2+} and cross-link with each other.[60] Very recently, GO films cross-linked by borate have been reported. With the introduction of 0.94 wt% boron in final GO film, the stiffness and strength of such films increase by over 255% and 20%, respectively. Such remarkable enhancements arise from the formation of covalent bonds between borate ions and the hydroxyl groups on the GO nanosheet (**Fig. 9**).[88] In addition, inspired by unique structure of natural nacre, Cheng *et al.*[89] synthesized ultratough highly conjugated cross-linked GO films by π-conjugated long-chain polymers made of 10,12-pentacosadiyn-1-ol (PCDO) monomers. PCDO monomers act as the "connectors", combining with adjacent GO sheets. But from a different prospective in our case, the long-chain polymer of PCDO could potentially tune the intersheets spacing and thereby improve the separation performance of GO based membranes. Of course, there are several interesting studies focusing on the functionalization of single-layered GO sheets and enhance the mechanical strength of GO films, including polyallylamine[90] or alkylamine functionalization[91], hydrogen bonding[92] and π-π interactions[93]. In a brief, those all offer promising possibilities to obtain high-performance GO membranes for separation applications.

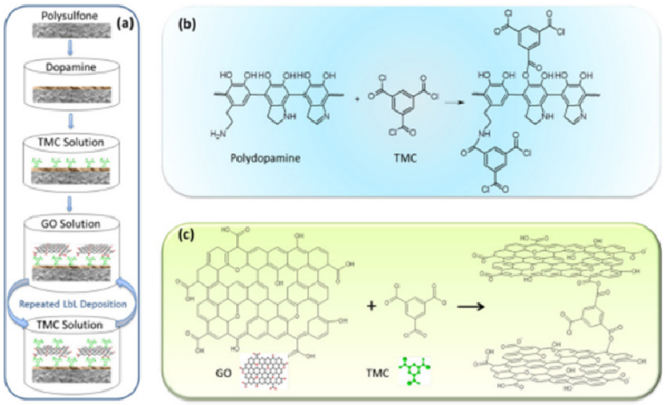

Fig. 10. *Schematic illustration of (a) a step-by-step procedure to synthesize the GO membrane, (b) the mechanism of reactions between polydopamine and TMC, and (c) the mechanism of reactions between GO and TMC. Reproduced from Ref. 94 with permission from American Chemical Society.*

Hu *et al.*[94] first assembled GO films via a layer-by-layer approach on a polydopamine-coated polysulfone support and then cross-linked them by 1,3,5-benzenetricarbonyl trichloride for separation purpose. The specific preparation processes can be seen in **Fig. 10**. Such membranes are still hydrophilic with an average water contact angle of 60º slightly larger than 30º of pristine GO membranes. The results of separation test of as-prepared chemically cross-linked GO membranes indicate that the pemeance of water decreases from 27.6 L m^{-2} h^{-1} bar^{-1} to 8.4 L m^{-2} h^{-1} bar^{-1} when the layers of GO sheets increase from 5 to 50 (**Fig. 11a**). Apparently, the water permeance of cross-linked GO

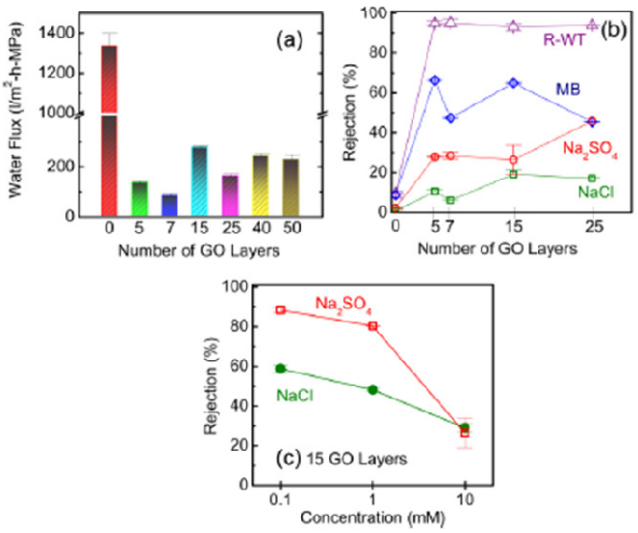

membranes is much smaller than 71 L m^{-2} h^{-1} bar^{-1} of pristine micrometer-thick GO membranes. This is due to the fact that the force of covalent bonds formed between these oxygen-containing functionalized groups and the small organics is much stronger than van der Waals forces and hydrogen bonds in fully wetted pristine GO membranes. Therefore, the intersheet spacing of cross-linked GO membranes is proposed to be smaller than that of pristine GO membrane. The latter rejection tests of ions and small dye molecules (**Fig. 11 b and c**) indicate that cross-linked

Fig. 11 *(a) water flux with different numbers of GO layers, (b) rejection of salts and organic dyes with different numbers of GO layers, and (c) effect of salt concentration on the rejection by the 15-layered GO membrane. The data at 0 layer are those of the polydopamine-coated membrane. All flux and rejection tests were performed under 50 psi (0.34 MPa). The rejection tests in (b) were performed with 20 mM NaCl, 10 mM Na_2SO_4, 7.5 mg/L MB, and 7.5 mg/L R-WT solutions, respectively. Reproduced from Ref. 94 with permission from American Chemical Society.*

GO membranes present relatively better selectivity of soluble salts, including NaCl and Na_2SO_4, because these ions can freely pass through fully wetted pristine GO membranes, suggesting that the intercalated small organics can not only effectively narrow the intersheet spacing, but act as barriers within GO membranes to form new nanochannels. This provides us a clue that if we engineer the size of these "connectors" between adjacent GO sheets, we can readily control the effective pore size of nanochannels with GO membranes by chemically modifying GO sheets with different organics at these active sites on GO sheets, which is similar to other carbon materials such as carbon nanotubes and graphene. With these exceptional properties, chemically cross-linked GO becomes an ideal candidate for potentially making high-performance membranes for water separation.

4.3 Nanostrand-channeled graphene oxide ~~GO~~ membrane

The nanostrand-channeling concept is demonstrated to be an effective technique to attain porous structure in membrane assembling.[5, 95-97] Very recently, Huang *et al.*[46] reported that nanostand-channeled GO (NSC-GO) membranes were successfully prepared by using copper hydroxide nanostands as

sacrifice templates. The $Cu(OH)_2$ nanostrand of 2.5 nm in diameter and micrometers in length can readily form stable aqueous solution because of its positive surface charges. When mixed with negatively charged GO sheets, $Cu(OH)_2$ nanostands would tightly combine with GO sheets by electrostatic attraction. The specific processes of assembling NSC-GO membranes can be seen in **Fig. 12**. A network of nanochannels with a narrow size distribution (3–5 nm) is formed when nanostands are removed by the acid solution. The water permeance of such membranes offers a 10-fold enhancement without sacrificing the rejection rate compared with that of pristine GO membranes, and is more than 100 times higher than that of commercial ultrafiltration membranes with similar rejection. In addition, these newly formed and well-defined nanochannels prepared by this nanostrand-channeling approach are likewise of excellent mechanical properties when loaded applied pressure. The dependence of separation performance on applied pressure is shown in **Fig. 13**. Note that the elastic deformation of the nanochannels depending on applied pressure leads to an abnormal phenomenon in separation performance (**Fig. 13a**), providing enormous possibilities in controlling permeance and rejection rate, particularly in pressure-driven separation application. Besides, the deformed nanochannels can quickly restore to the original state based on MD simulations results.

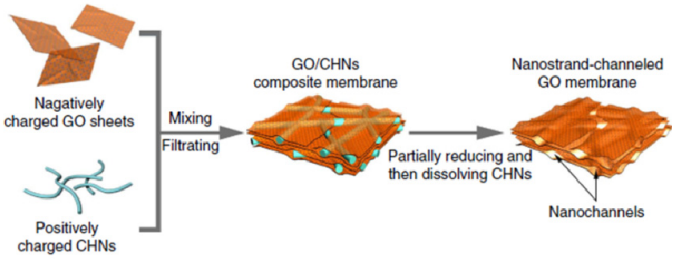

Fig. 12. *Illustration of the fabrication process of NSC-GO membrane. A multi-step process consisting of formation of a dispersion of positively charged copper hydroxide nanostrands (CHNs) and negatively charged GO sheets on a porous support, followed by hydrazine reduction, and finally CHN removal. Reproduced from Ref. 46 with permission from Nature Publishing Group.*

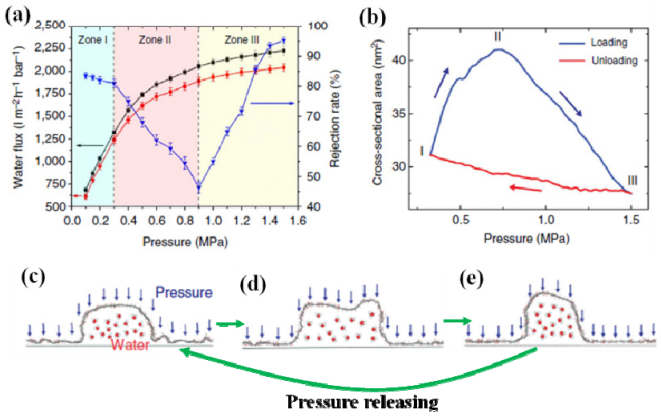

Fig. 13. *(a) Pressure-dependent flux and rejection of EB molecules of NSC-GO membrane under different pressure. The black solid squares and red solid circles curve represent the flux variation during the first and third pressure-loading processes, respectively. The blue solid triangle curve denotes the rejection rate of EB during the first pressure-loading process. All the error bars are average errors from five measurement data. (b) Simulated changes in the cross-sectional area of nanochannel by varying the applied pressure. (c–e) The response of a half cylindrical GO nanochannel modeled in MD simulation. Adapted from Ref. 46 with permission from Nature Publishing Group.*

5. Conclusions and outlook

In summary, laminar GO membranes emerge as a new star for ultrafast permeance, excellent mechanical strength and energy-efficient membranes for precise gas selectivity, ionic and molecular sieving in aqueous solution, as well as applications in other important fields. In this review, the structure and preparation of GO membranes have been briefly summarized. Emphasis are mainly placed on the applications of GO membranes in gas separation, ions selectivity and small molecules sieving as well as the latest progress on enhancing the separation performance of GO membranes, including the assembly of nanoporous GO membranes, chemically cross-linked GO membranes and nanostand-channeled GO membranes. Note that several explorations of nanoporous GO sheets highlight great possibilities of preparing a series of nanoporous GO membranes with well-defined nanochannels for industrial separation applications. Further works are needed to address the issues of the variations of surface charges and hydrophilic property of chemical modified single-layer GO sheets. These two factors have critical impacts on fabricating uniform GO membranes by the techniques of vacuum filtration, spin-coating and so on.

Nonetheless, high-performance GO membrane is still a "beacon", representing the next class of multifunctional membranes in ultrafiltration and nanofiltration applications. It can't be denied that there are still several unexplored fields toward the wider application of GO membranes in separation application such as improving the stability of fully wetted GO membranes in cross-flow conditions.

Notes and references

[a] *State Key Laboratory of Silicon Materials, Department of Materials Science and Enginnering, Zhejiang University, Hangzhou 310027, China E-mail: pengxinsheng@zju.edu.cn*
[b] *Cyrus Tang Centre for Sensor Materials and Applications, Zhejiang University, Hangzhou 310027, China.*
Acknowledgement: *This work was supported by National Nature Science Foundations of China (NSFC 21271154), and Doctoral Fund of Ministry of Education of China (20110101110028), Natural Science Foundation for Outstanding Young Scientist of Zhejiang Province (LR14E020001).*
† Electronic Supplementary Information (ESI) available: [details of any supplementary information available should be included here]. See DOI: 10.1039/b000000x/

1 M. A. Shannon, P. W. Bohn, M. Elimelech, J. G. Georgiadis, B. J. Mariñas and A. M. Mayes, *Nature*, 2008, **452**, 301-310.
2 N. Savage and M. S. Diallo, *J. Nanopart. Res.*, 2005, **7**, 331-342.
3 X. Zhang, T. Zhang, J. Ng and D. D. Sun, *Adv. Funct. Mater.*, 2009, **19**, 3731-3736.
4 B. Van der Bruggen, C. Vandecasteele, T. Van Gestel, W. Doyen and R. Leysen, *Environ. Progress*, 2003, **22**, 46-56.
5 X. Peng, J. Jin, Y. Nakamura, T. Ohno and I. Ichinose, *Nat. Nanotechn.*, 2009, **4**, 353-357.

6. R. Van Reis and A. Zydney, *Current Opinion in Biotechn.,* 2001, **12**, 208-211.
7 L. Yan, Y. S. Li and C. B. Xiang, *Polymer*, 2005, **46**, 7701-7706.
8 Z.-L. Xu and F. Alsalhy Qusay, *J. Membr. Sci.*, 2004, **233**, 101-111.
9 B. Van der Bruggen, M. Mänttäri and M. Nyström, *Separat. Purif. Techn.*, 2008, **63**, 251-263.
10 M. Ulbricht, *Polymer*, 2006, **47**, 2217-2262.
11 M. Mulder, *Basic Principles of Membrane Technology Second Edition*, Kluwer Academic Pub, 1996.
12 K. M. Persson, V. Gekas and G. Trägårdh, *J. Membr. Sci.*, 1995, **100**, 155-162.
13 K. Scott, *Handbook of industrial membranes*, Elsevier, 1995.
14 H. Choi, E. Stathatos and D. D. Dionysiou, *Applied Catalysis B-Environmental*, 2006, **63**, 60-67.
15 K. Shqau, M. L. Mottern, D. Yu and H. Verweij, *J. Am. Ceram. Soc.*, 2006, **89**, 1790-1794.
16 T. Van Gestel, C. Vandecasteele, A. Buekenhoudt, C. Dotremont, J. Luyten, R. Leysen, B. Van der Bruggen and G. Maes, *J. Membr. Sci.*, 2002, **207**, 73-89.
17 T. Matsuura, *Synthetic membranes and membrane separation processes*, CRC press, 1993.
18 S. Benfer, U. Popp, H. Richter, C. Siewert and G. Tomandl, *Separation and purification technology*, 2001, **22**, 231-237.
19 J. Robertson, *Materials Science and Engineering: R: Reports*, 2002, **37**, 129-281.
20 M. F. De Volder, S. H. Tawfick, R. H. Baughman and A. J. Hart, *Science*, 2013, **339**, 535-539.
21 A. Kalra, S. Garde and G. Hummer, *Proc. Nat. Academ. Sci.*, 2003, **100**, 10175-10180.
22. J. K. Holt, H. G. Park, Y. Wang, M. Stadermann, A. B. Artyukhin, C. P. Grigoropoulos, A. Noy and O. Bakajin, *Science*, 2006, **312**, 1034-1037.
23 S. Karan, S. Samitsu, X. Peng, K. Kurashima and I. Ichinose, *Science*, 2012, **335**, 444-447.
24 R. Nair, H. Wu, P. Jayaram, I. Grigorieva and A. Geim, *Science*, 2012, **335**, 442-444.
25 D. R. Paul, *Science*, 2012, **335**, 413-414.
26 M. Majumder, N. Chopra and B. J. Hinds, *ACS nano*, 2011, **5**, 3867-3877.
27 H. Verweij, M. C. Schillo and J. Li, *Small*, 2007, **3**, 1996-2004.
28 M. Majumder, N. Chopra, R. Andrews and B. J. Hinds, *Nature*, 2005, **438**, 44-44.
29 S. Joseph and N. Aluru, *Nano Lett.*, 2008, **8**, 452-458.
30 G. Hummer, J. C. Rasaiah and J. P. Noworyta, *Nature*, 2001, **414**, 188-190.
31 S. Li, H. Li, X. Wang, Y. Song, Y. Liu, L. Jiang and D. Zhu, *J. Phys. Chem. B*, 2002, **106**, 9274-9276.
32 D. R. Paul, *Science*, 2012, **335**, 413-414.
33 A. Voevodin and M. Donley, *Surf. Coat. Techn.*, 1996, **82**, 199-213.
34 S. P. Koenig, L. Wang, J. Pellegrino and J. S. Bunch, *Nat. Nanotechn.*, 2012, **7**, 728-732.
35 S. Garaj, W. Hubbard, A. Reina, J. Kong, D. Branton and J. Golovchenko, *Nature*, 2010, **467**, 190-193.
36 D. Cohen-Tanugi and J. C. Grossman, *Nano letters*, 2012, **12**, 3602-3608.
37 D.-E. Jiang, V. R. Cooper and S. Dai, *Nano Lett.*, 2009, **9**, 4019-4024.
38 M. E. Suk and N. Aluru, *J. Phys. Chem. Lett.*, 2010, **1**, 1590-1594.
39 G. F. Schneider, S. W. Kowalczyk, V. E. Calado, G. Pandraud, H. W. Zandbergen, L. M. Vandersypen and C. Dekker, *Nano Lett.*, 2010, **10**, 3163-3167.
40 D. Li, M. B. Mueller, S. Gilje, R. B. Kaner and G. G. Wallace, *Nat. Nanotechn.*, 2008, **3**, 101-105.
41 O. C. Compton and S. T. Nguyen, *Small*, 2010, **6**, 711-723.
42 K. Raidongia and J. Huang, *J. Am. Chem. Soc.*, 2012, **134**, 16528-16531.
43 P. Sun, M. Zhu, K. Wang, M. Zhong, J. Wei, D. Wu, Z. Xu and H. Zhu, *ACS Nano*, 2012, **7**, 428-437.
44 R. Joshi, P. Carbone, F. Wang, V. Kravets, Y. Su, I. Grigorieva, H. Wu, A. Geim and R. Nair, *arXiv preprint arXiv:1401.3134*, 2014.
45 L. Qiu, X. Zhang, W. Yang, Y. Wang, G. P. Simon and D. Li, *Chem. Commun.*, 2011, **47**, 5810-5812.
46 H. Huang, Z. Song, N. Wei, L. Shi, Y. Mao, Y. Ying, L. Sun, Z. Xu and X. Peng, *Nat. Commun*, 2013, **4**, 2979.
47 H. Huang, Y. Mao, Y. Ying, Y. Liu, L. Sun and X. Peng, *Chem. Commun.*, 2013, **49**, 5963-5965.
48 B. Mi, *Science*, 2014, **343**, 740-742.
49 H. He, J. Klinowski, M. Forster and A. Lerf, *Chem. Phys. Lett.*, 1998, **287**, 53-56.
50 D. R. Dreyer, S. Park, C. W. Bielawski and R. S. Ruoff, *Chem. Soc. Rev.*, 2010, **39**, 228-240.
51 D. A. Dikin, S. Stankovich, E. J. Zimney, R. D. Piner, G. H. Dommett, G. Evmenenko, S. T. Nguyen and R. S. Ruoff, *Nature*, 2007, **448**, 457-460.
52 C. K. Chua, M. Pumera, *Chem. Soc. Rev.,* 2014, **43**, 291-312.
53 K. A. Mkhoyan, A. W. Contryman, J. Silcox, D. A. Stewart, G. Eda, C. Mattevi, S. Miller and M. Chhowalla, *Nano Lett.*, 2009, **9**, 1058-1063.
54 P. Sun, F. Zheng, M. Zhu, Z. Song, K. Wang, M. Zhong, D. Wu, R. Little, Z. Xu and H. Zhu, *ACS nano*, 2014, **8**, 850-859.
55 V. H. Pham, T. V. Cuong, S. H. Hur, E. W. Shin, J. S. Kim, J. S. Chung, E. J. Kim, *Carbon*, 2010, **48**, 1945-1951.
56 C. Xu, X. Wu, J. Zhu and X. Wang, *Carbon*, 2008, 46, 386-389.
57 X. Wang, H. Bai and G. Shi, *J. Am. Chem. Soc.*, 2011, **133**, 6338-6342.
58 K. W. Putz, O. C. Compton, C. Segar, Z. An, S. T. Nguyen and L. C. Brinson, *ACS Nano*, 2011, **5**, 6601-6609.
59 X. Yang, L. Qiu, C. Cheng, Y. Wu, Z. F. Ma and D. Li, *Angew. Chem. Int. Edit.*, 2011, **50**, 7325-7328.
60 S. Park, K.-S. Lee, G. Bozoklu, W. Cai, S. T. Nguyen and R. S. Ruoff, *ACS Nano*, 2008, **2**, 572-578.
61 J. W. Suk, R. D. Piner, J. An and R. S. Ruoff, *ACS nano*, 2010, **4**, 6557-6564.
62 Y. Han, Z. Xu and C. Gao, *Adv. Funct. Mater.*, 2013, 23, 3693-3700.
63 J. S. Bunch, S. S. Verbridge, J. S. Alden, A. M. van der Zande, J. M. Parpia, H. G. Craighead and P. L. McEuen, *Nano Lett.*, 2008, **8**, 2458-2462.
64 D. W. Boukhvalov, M. I. Katsnelson and Y.-W. Son, *Nano Lett.*, 2013, **13**, 3930-3935.
65 H. W. Kim, H. W. Yoon, S.-M. Yoon, B. M. Yoo, B. K. Ahn, Y. H. Cho, H. J. Shin, H. Yang, U. Paik and S. Kwon, *Science*, 2013, **342**, 91-95.
66 S. Adhikari and S. Fernando, *Indust. Eng. Chem. Res.*, 2006, **45**, 875-881.
67 H. B. Park, C. H. Jung, Y. M. Lee, A. J. Hill, S. J. Pas, S. T. Mudie, E. Van Wagner, B. D. Freeman and D. J. Cookson, *Science*, 2007, **318**, 254-258.
68 I. Pinnau and W. J. Koros, *Indust. Eng. Chem.Res.*, 1991, **30**, 1837-1840.
69 K. Kusakabe, T. Kuroda and S. Morooka, *J.Membr.Sci.*, 1998, **148**, 13-23.
70 H. Li, Z. Song, X. Zhang, Y. Huang, S. Li, Y. Mao, H. J. Ploehn, Y. Bao and M. Yu, *Science*, 2013, **342**, 95-98.
71 N. W. Ockwig and T. M. Nenoff, *Chem. Rev.*, 2007, **107**, 4078-4110.
72 H. Du, J. Li, J. Zhang, G. Su, X. Li and Y. Zhao, *J. Phys. Chem. C*, 2011, **115**, 23261-23266.
73 S. Blankenburg, M. Bieri, R. Fasel, K. Müllen, C. A. Pignedoli and D. Passerone, *Small*, 2010, **6**, 2266-2271.
74 J. Schrier, *J. Phys. Chem. Lett.*, 2010, **1**, 2284-2287.
75 A. W. Hauser and P. Schwerdtfeger, *J. Phys. Chem. Lett.*, 2012, **3**, 209-213.
76 K. Sint, B. Wang and P. Král, *J. Am. Chem. Soc.*, 2008, **130**, 16448-16449.
77 X. Li, W. Cai, J. An, S. Kim, J. Nah, D. Yang, R. Piner, A. Velamakanni, I. Jung and E. Tutuc, *Science*, 2009, **324**, 1312-1314.
78 X. Li, C. W. Magnuson, A. Venugopal, R. M. Tromp, J. B. Hannon, E. M. Vogel, L. Colombo and R. S. Ruoff, *J. Am. Chem. Soc.*, 2011, **133**, 2816-2819.
79 A. Reina, X. Jia, J. Ho, D. Nezich, H. Son, V. Bulovic, M. S. Dresselhaus and J. Kong, *Nano Lett.*, 2008, **9**, 30-35.
80 M. D. Fischbein and M. Drndić, *Appl. Phys. Lett.*, 2008, **93**, 113107.

81 J. Cai, P. Ruffieux, R. Jaafar, M. Bieri, T. Braun, S. Blankenburg, M. Muoth, A. P. Seitsonen, M. Saleh and X. Feng, *Nature*, 2010, **466**, 470-473.

82 M. Bieri, M. Treier, J. Cai, K. Aït-Mansour, P. Ruffieux, O. Gröning, P. Gröning, M. Kastler, R. Rieger and X. Feng, *Chem. Ccommun.*, 2009, 6919-6921.

83 M. Kim, N. S. Safron, E. Han, M. S. Arnold and P. Gopalan, *Nano Lett.*, 2010, **10**, 1125-1131.

84 C. A. Merchant, K. Healy, M. Wanunu, V. Ray, N. Peterman, J. Bartel, M. D. Fischbein, K. Venta, Z. Luo and A. C. Johnson, *Nano Lett.*, 2010, **10**, 2915-2921.

85 Y. Zhu, S. Murali, M. D. Stoller, K. Ganesh, W. Cai, P. J. Ferreira, A. Pirkle, R. M. Wallace, K. A. Cychosz and M. Thommes, *Science*, 2011, **332**, 1537-1541.

86 J. G. Radich and P. V. Kamat, *ACS nano*, 2013, **7**, 5546-5557.

87 Y. Ying, L. Sun, Q. Wang, Z. Fan, X. Peng, *RSC Adv. 2014,* **4**, 21425-21428.

88 Z. An, O. C. Compton, K. W. Putz, L. C. Brinson and S. T. Nguyen, *Adv. Mater.*, 2011, **23**, 3842-3846.

89 Q. Cheng, M. Wu, M. Li, L. Jiang and Z. Tang, *Angew.Chem. Int. Edt.*, 2013, **52**, 3750-3755.

90 S. Park, D. A. Dikin, S. T. Nguyen and R. S. Ruoff, *J. Phys. Chem. C*, 2009, **113**, 15801-15804.

91 S. Stankovich, D. A. Dikin, O. C. Compton, G. H. Dommett, R. S. Ruoff and S. T. Nguyen, *Chem. Mater.*, 2010, **22**, 4153-4157.

92 O. C. Compton, S. W. Cranford, K. W. Putz, Z. An, L. C. Brinson, M. J. Buehler and S. T. Nguyen, *ACS nano*, 2012, **6**, 2008-2019.

93 Y. Xu, H. Bai, G. Lu, C. Li and G. Shi, *J.Am. Chem. Soc.*, 2008, 130, 5856-5857.

94 M. Hu and B. Mi, *Environ. Sci. Ttechn.*, 2013, **47**, 3715-3723.

95 L. Shi, Q. Yu, Y. Mao, H. Huang, H. Huang, Z. Ye and X. Peng, *J. Mater. Chem.*, 2012, **22**, 21117-21124.

96 L. Shi, H. Huang, L. Sun, Y. Lu, B. Du, Y. Mao, J. Li, Z. Ye and X. Peng, *Dalton Transact.*, 2013, **42**, 13265-13272.

97 L. Shi, Q. Yu, H. Huang, Y. Mao, J. Lei, Z. Ye and X. Peng, *J. Mater. Chem. A*, 2013, **1**, 1899-1906.

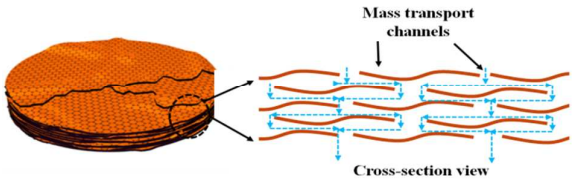

Due to their unique phyisical and chemical properties, graphene oxide nanosheets repersnt an emerging star material for novel separation membranes.